Electronic Supplementary Material (ESI) for Materials Horizons.
This journal is © The Royal Society of Chemistry 2017

Supporting Information

Title: An All-Solid-State Biocompatible Ion-to-Electron Transducer for Bioelectronics

Margarita Sheliakina, A. Bernardus Mostert, Paul Meredith

S1. Capacitance Calculations

If we consider that melanin and PEDOT:PSS form two capacitors in series, then the total capacitance of the system is given by:

$$\frac{1}{C_{tot}} = \frac{1}{C_m} + \frac{1}{C_p} \tag{S1}$$

Where *tot* indicates the total value, *m* is for melanin and *p* is for the PEDOT:PSS. We can rewrite the above to account for the volumetric capacitances and the volumes of the materials:

$$\frac{1}{C_{tot}} = \frac{1}{C_m^* xyt} + \frac{1}{C_p^* xyd} \tag{S2}$$

where xy is the area of the electrical contacts, d is the PEDOT:PSS thickness and t is the melanin thickness, C_m^* is the volumetric capacitance of melanin and C_p^* is the volumetric capacitance of the PEDOT:PSS. The above can be normalized to contact surface area as follows:

$$\frac{xy}{C_{tot}} = \frac{1}{C_m^* t} + \frac{1}{C_p^* d} \tag{S3}$$

Which is the equation modelled in Fig. 4b. Essentially, since the melanin thickness does not change, the equation shows that one can expect the left side to vary linearly with $1/d$.

S2. OECT Modelling

The original model for understanding liquid based OECTs was developed by Barnards *et al.*[SR1] and Rivnay *et al.*[SR2] Below is an amendment to account for the melanin top gate which requires knowledge of how much protonic charge is in the PEDOT:PSS (assuming that the melanin is the proton source).

Given the comproportionation reaction (Fig. 1 of the main manuscript), it follows that the number of protons, from melanin, in PEDOT:PSS is equal to the number of semiquinone anions (SQ-) stabilized at a given voltage. As such we can assume, under steady state conditions, that melanin is a capacitor stabilizing SQ- ions and PEDOT:PSS a capacitor housing protons. Therefore, at steady state, the total gate voltage across the device is given by:

$$V_g = V_m + V_p \tag{S4}$$

Where *m* denotes melanin and *p* PEDOT:PSS. Applying Kirchhoff's laws we can state that the charge on both capacitors are equal, thus:

$$V_g = -\frac{Q}{C_m} + \frac{Q}{C_p} \tag{S5}$$

Where the negative sign indicates the negative charge of the semiquinone anion. Given that the number of semiquinone anions equal the number of protons, one can write:

$$V_g = eN_H\left(-\frac{1}{C_m} + \frac{1}{C_p}\right) \tag{S6}$$

Where *e* is the fundamental charge, and N_H is the number of protons. Rearranging:

$$N_H = \frac{V_g}{e\left(-\frac{1}{C_m^* WLt} + \frac{1}{C_p^* WLd}\right)} \tag{S7}$$

Where *W* is width of channel, *L* is length of the channel, *d* is thickness of PEDOT:PSS and *t* is thickness of melanin, and the * indicates volumetric capacitance. Continuing the derivation:

$$N_H = \frac{V_g}{\frac{e}{WL}\left(-\frac{1}{C_m^* t} + \frac{1}{C_p^* d}\right)} \tag{S8}$$

$$N_H = \frac{V_g WL}{e\left(-\frac{1}{C_m^* t} + \frac{1}{C_p^* d}\right)} \tag{S9}$$

$$N_H = \frac{V_g WL}{e\left(\frac{C_m^* t - C_p^* d}{C_m^* t C_p^* d}\right)} \tag{S10}$$

$$N_H = \frac{V_g WL C_m^* t C_p^* d}{e\left(C_m^* t - C_p^* d\right)} \tag{S11}$$

The density of charges in the PEDOT:PSS can be written as:

$$n_H = \frac{V_g C_m^* t C_p^*}{e\left(C_m^* t - C_p^* d\right)} \tag{S12}$$

Having derived the proton charge density in PEDOT:PSS, we can apply this new definition into the derivation of Bernards *et al.* and Rivnay *et al*. We begin with Ohm's law for the PEDOT:PSS channel:

$$I_d = Wde\mu p(x)\frac{dV(x)}{dx} \tag{S13}$$

Where μ is the hole mobility and $p(x)$ is the hole density in a given position x in the channel. The hole density is given by:

$$p(x) = [\mathrm{SO_3^-}] - H^+(x) \tag{S14}$$

where $[\mathrm{SO_3^-}]$ is the density of sulfonate groups that are compensated with holes in neat PEDOT:PSS, and $H^+(x)$ is the proton density. This proton density given the gate voltage and source drain voltage at a given point $x(V(x))$ is then given by:

$$H^+(x) = \frac{C_m^* t C_p^*}{e\left(C_m^* t - C_p^* d\right)} V_g - \frac{C_m^* t C_p^*}{e\left(C_m^* t - C_p^* d\right)} V(x) \tag{S15}$$

We now substitute this proton density into the hole density and Ohm's law:

$$I_d = Wde\mu \frac{dV(x)}{dx}\left([\mathrm{SO_3^-}] - \frac{C_m^* t C_p^*}{e\left(C_m^* t - C_p^* d\right)} V_g + \frac{C_m^* t C_p^*}{e\left(C_m^* t - C_p^* d\right)} V(x)\right) \tag{S16}$$

Let $\alpha = C^*_m t/(C^*_m t - C^*_p d)$, then we have:

$$I_d = Wd\mu\alpha C_p^* \frac{dV(x)}{dx}\left(\frac{e[\mathrm{SO}_3^-]}{\alpha C_p^*} - V_g + V(x)\right) \tag{S17}$$

Integrating:

$$I_d L = Wd\mu\alpha C_p^* \left(\frac{e[\mathrm{SO}_3^-]}{\alpha C_p^*} V_d - V_g V_d + \frac{V_d^2}{2}\right) \tag{S18}$$

where, L is the channel length and V_d is the source drain voltage. Continuing:

$$I_d = \frac{Wd\mu\alpha C_p^*}{L}\left(\frac{e[\mathrm{SO}_3^-]}{\alpha C_p^*} - V_g + \frac{V_d}{2}\right)V_d \tag{S19}$$

$$I_d = \frac{Wd\mu\alpha C_p^*}{L}\left(\frac{V_T}{\alpha} - V_g + \frac{V_d}{2}\right)V_d \tag{S20}$$

which is Equation 3. To obtain the saturation condition, we use $V_d = V_g - V_T/\alpha$ and substitute to obtain:

$$I_d = \frac{Wd\mu\alpha C_p^*}{L}\left(\frac{V_T}{\alpha} - V_g + \frac{V_g - \frac{V_T}{\alpha}}{2}\right)\left(V_g - \frac{V_T}{\alpha}\right) \tag{S21}$$

$$I_d = \frac{Wd\mu\alpha C_p^*}{L}\left(\frac{\frac{V_T}{\alpha} - V_g}{2}\right)\left(V_g - \frac{V_T}{\alpha}\right) \tag{S22}$$

$$I_d = \frac{Wd\mu\alpha C_p^*}{2L}\left(\frac{V_T}{\alpha} - V_g\right)\left(V_g - \frac{V_T}{\alpha}\right) \tag{S23}$$

$$I_d = -\frac{Wd\mu\alpha C_p^*}{2L}\left(\frac{V_T}{\alpha} - V_g\right)^2 \tag{S24}$$

which is the saturation current. Taking the derivative with respect to gate voltage yields the transconductance at saturation:

$$g_m = \frac{Wd\mu\alpha C_p^*}{L}\left(\frac{V_T}{\alpha} - V_g\right) \tag{S25}$$

which is Eq. 4.

S3. Supplementary Figures

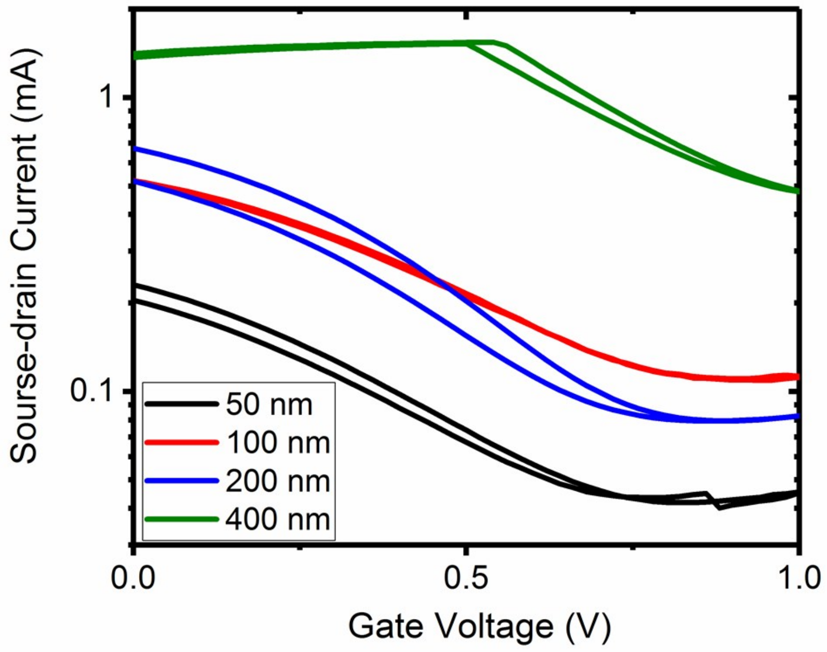

Fig. S1 Transfer characteristics as a function of channel thickness**.** Transfer characteristics for V_d^{SAT} at a V_g of 0 V for different PEDOT:PSS channel thickness. As one would expect the transfer curves are shifted to a higher I_d for thicker channels.

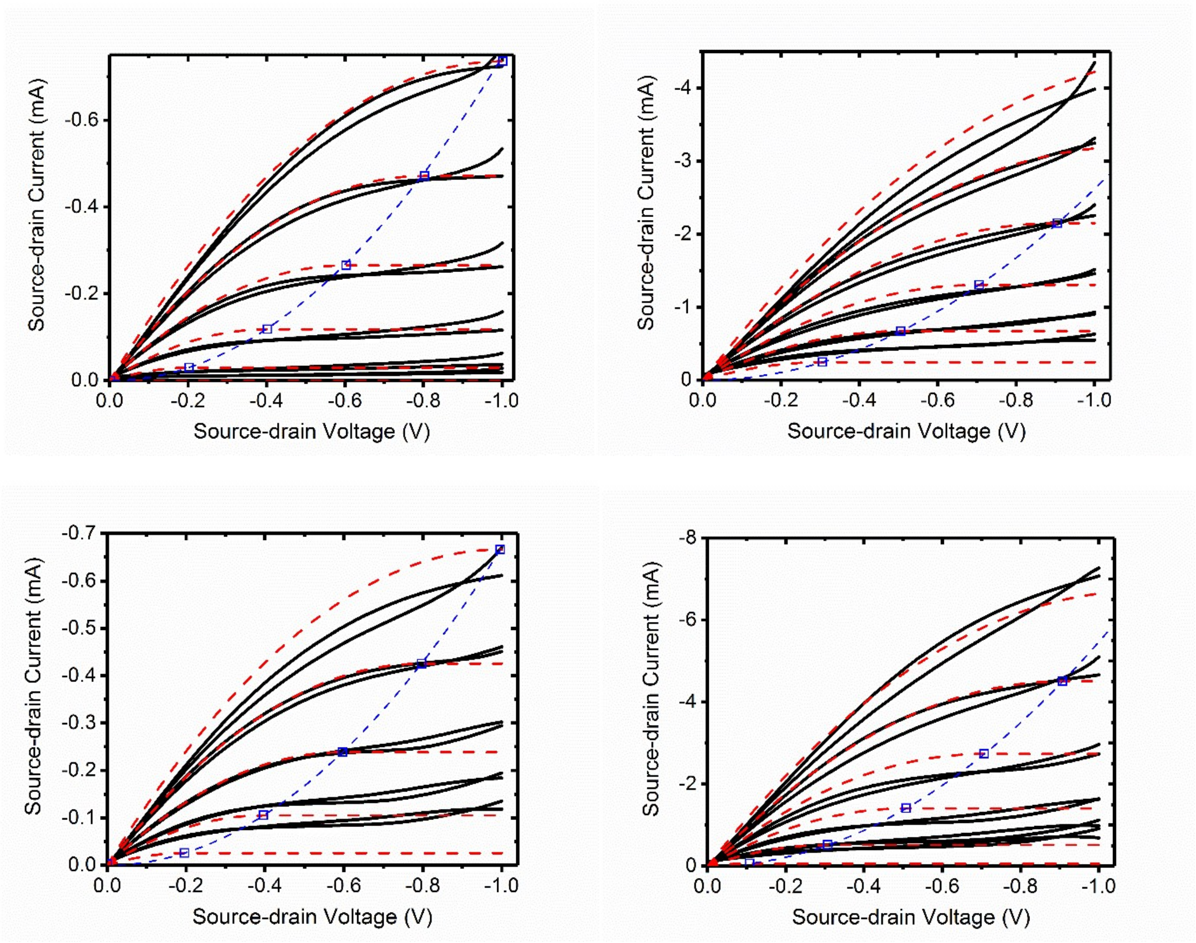

Fig. S2 Output characteristics as a function of channel thickness. Output characteristics of OECTs with 50 nm (a), 100 nm (b), 200 nm (c) and 400 (nm) thick channels (black lines), V_g = -0.2 to 0.8 V (top to bottom), with the corresponding fits (red dashed lines). Blue empty squares are the saturation values.

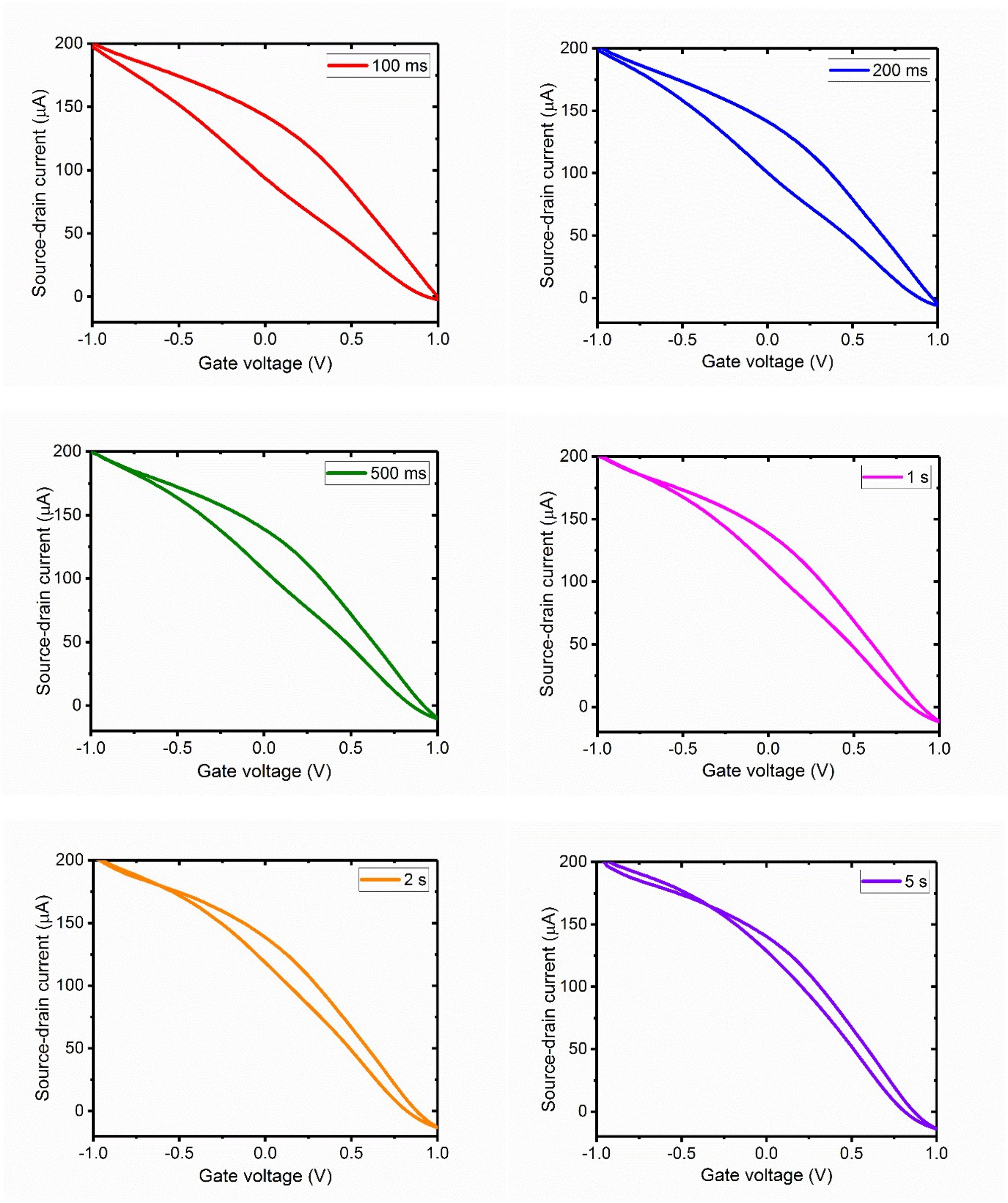

Fig. S3 Transfer characteristics as a function of measurement delay time. Transfer characteristics of a melanin-based OECT (100 nm channel thickness) measured at different delay times (time before data points). The source-drain voltage was 100 mV in all cases and the top contact was gold. It can be seen that the hysteresis decreases with increasing delay time which is a clear indication of the ionic nature of the charge in melanin.

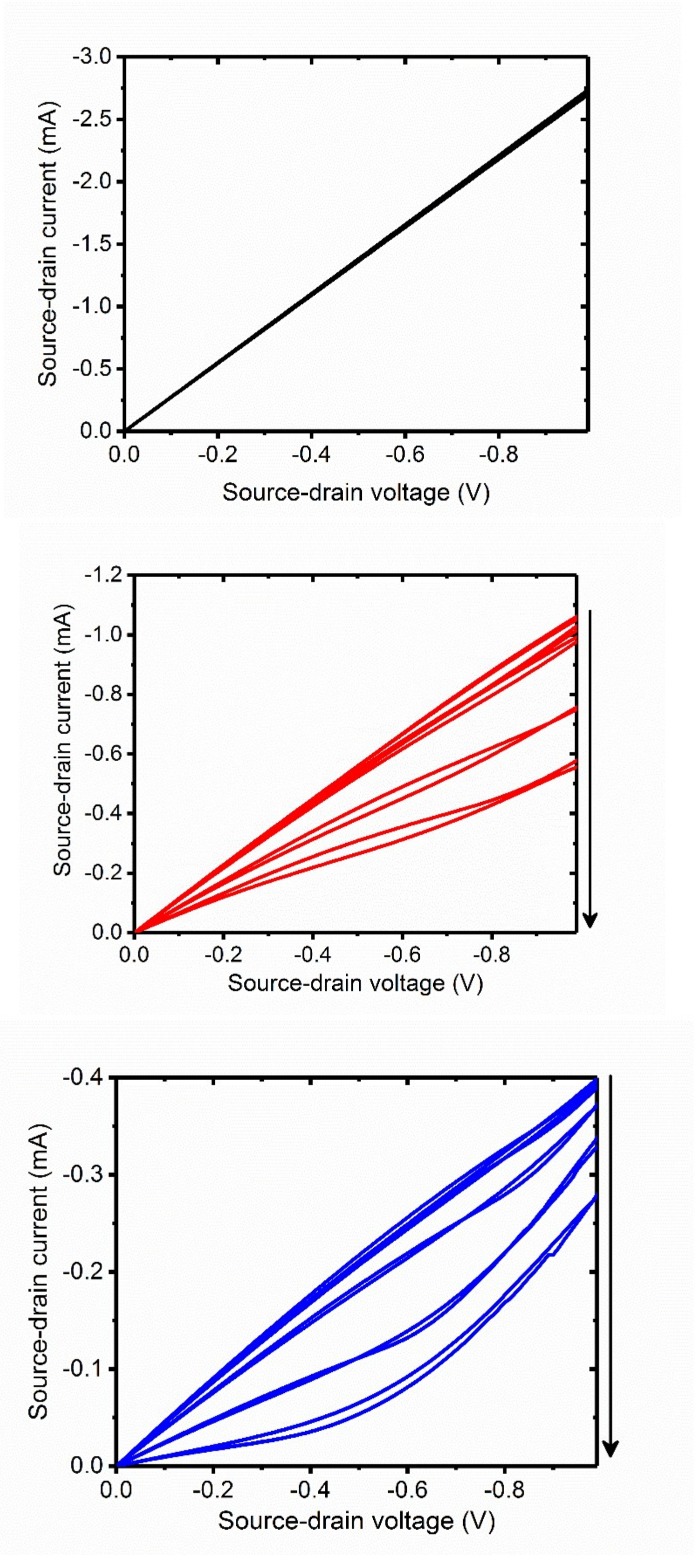

Fig. S4 Output characteristics as a function of hydration. Output characteristics of a typical OECT (100 nm channel thickness) with a liquid top gate (EGaIn) contact under negative bias at the drain and held at 0 mbar (a), 8 mbar (b) and 18 mbar (c). The arrows indicate the direction of the gate voltage being changed from -1 to 1 V with a step of 0.5 V. A positive gate bias de-dopes the channel and decreases the absolute value of the current. These output characteristics show *p*-type behavior.

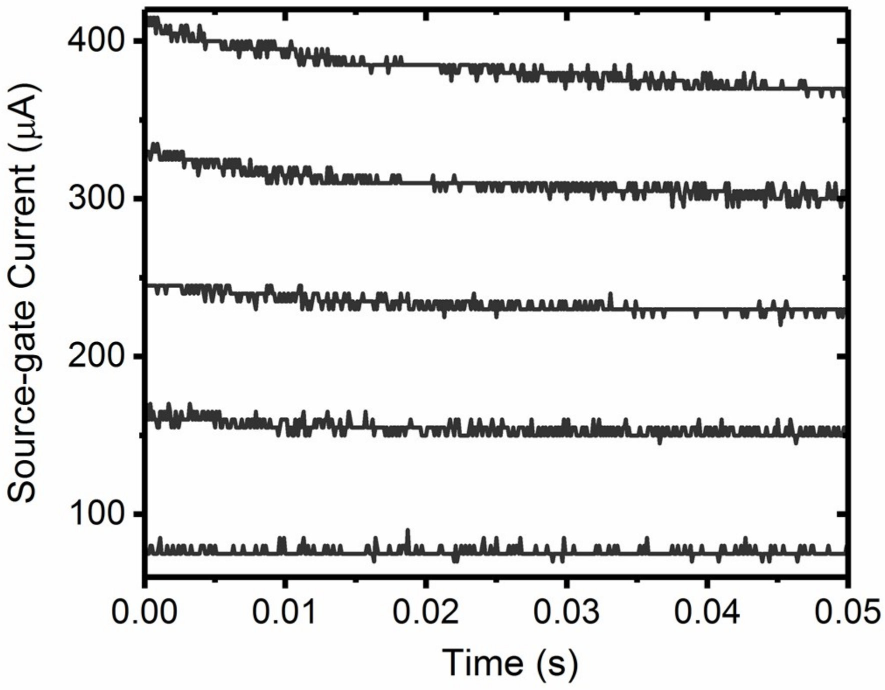

Fig. S5 An example of gate/drain current transient measurements. An example of the gate/drain current transient measurements from an OECT with channel thickness 50 nm, for different values of applied gate voltage (0.2 V to 1 V bottom to top). From this data the total amount of charge injected at a given gate voltage can be determined as well as the capacitance of the devices, as presented in Fig. 4.

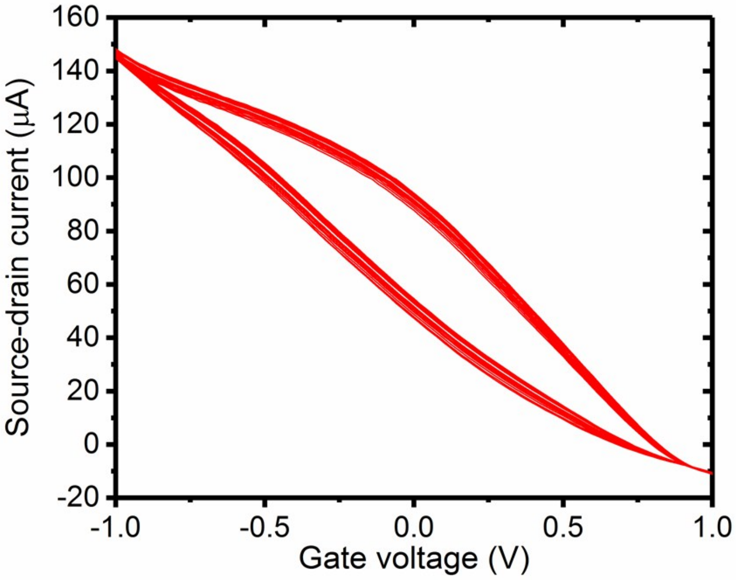

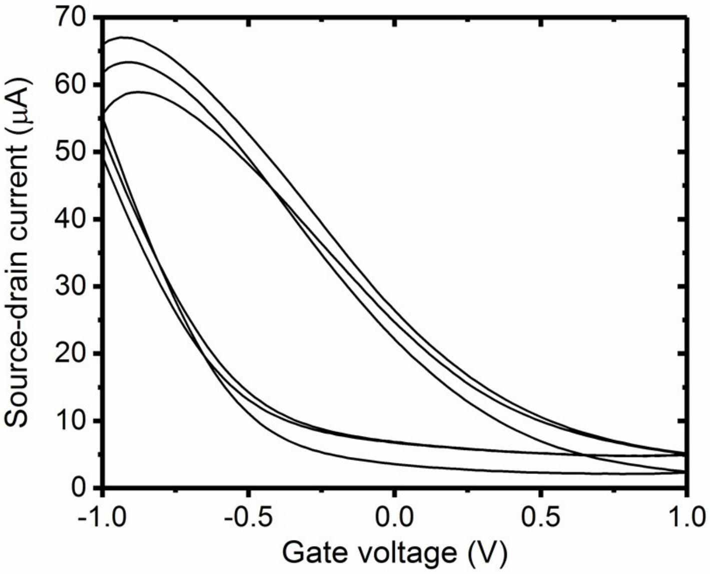

Fig. S6 Reproducibility curves of a melanin-based OECT. Reproducibility of a melanin-based OECT with a gold top gate contact (a), and an EGaIn top-gate electrode (b). For both types of devices very good reproducibility was achieved. For a gold-contact OECT each transfer curve was measured 2 min after the previous. For the EGaIn-electrode device each transfer curve was measured after lifting the sample up and lowering it back down to create the same contact area.

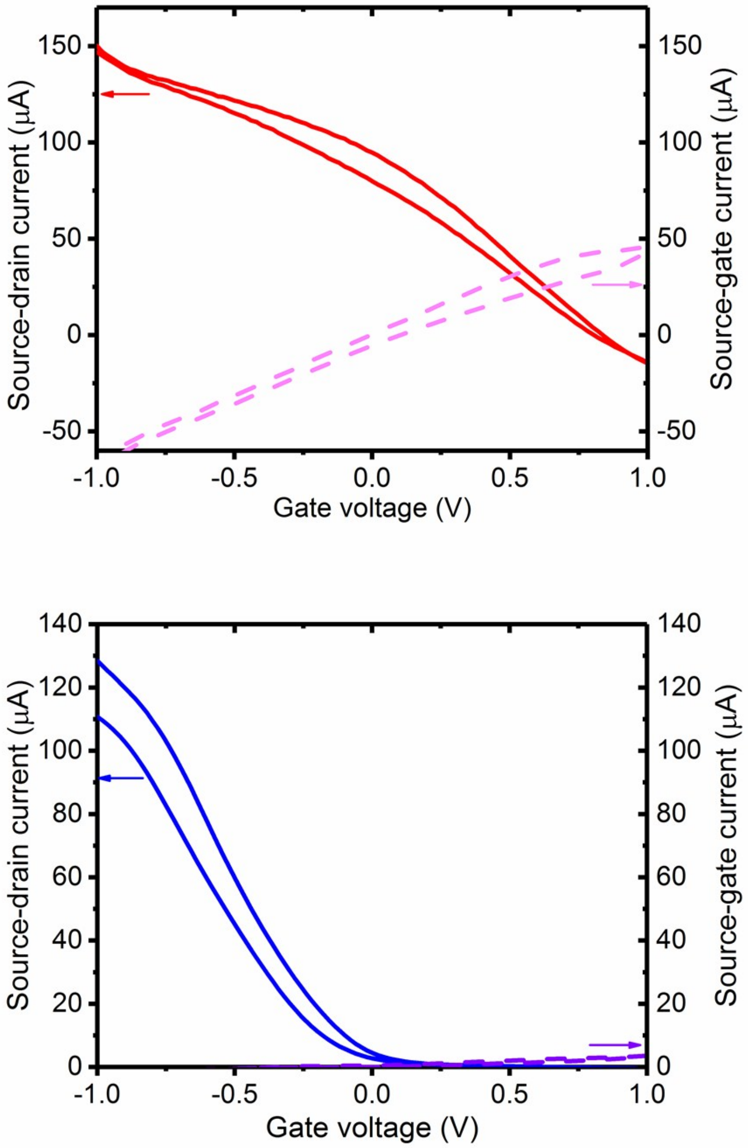

Fig. S7 Source-gate leakage current examples. Source-gate leakage current for a gold top gate contact (a), and an EGaIn top gate contact (b) OECT. It can be seen that using a liquid gate contact decreased the source-gate leakage by almost an order of magnitude. The gold contact evaporated on the melanin gate surface partially blocks water penetration through the film.

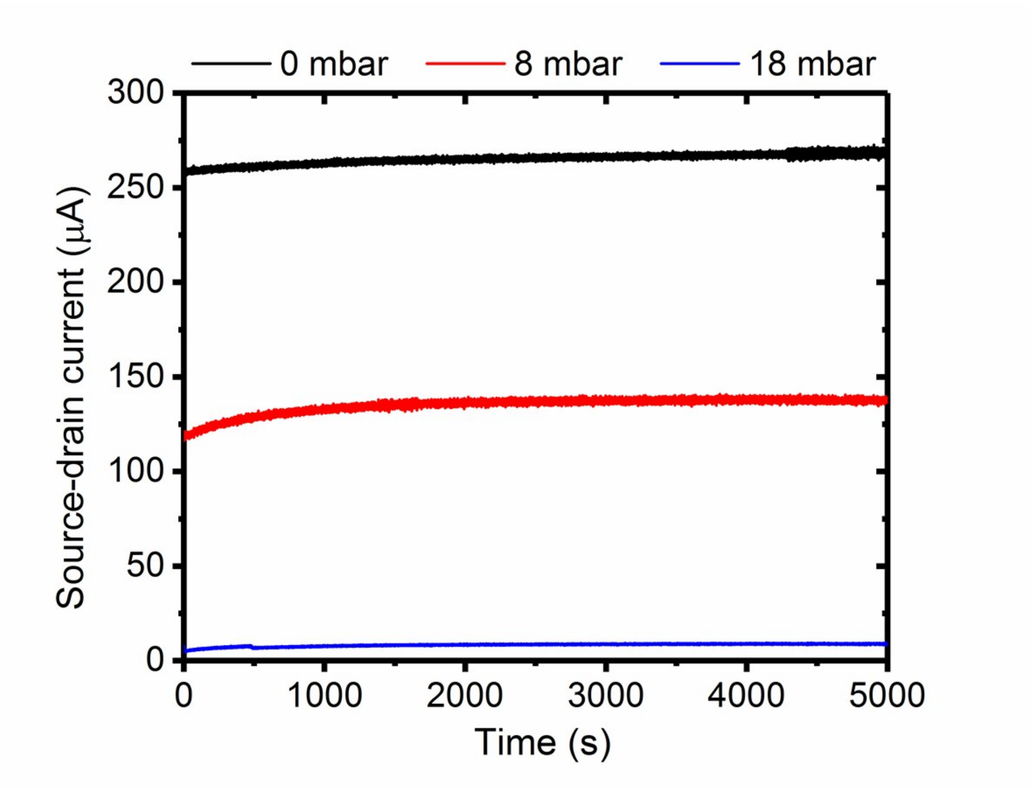

Fig. S8 Time dependent current measurements for an OECT. Time dependent current measurements for an OECT exposed to a wet atmosphere and without the EGaIn top contact. Adsorption isotherm measurements[SR3,SR4] previously demonstrated that at least an hour is required to achieve equilibrium water content in melanin pressed powder pellets and films. To ensure equilibrium hydration conditions, a time dependent current measurement was taken before each of the pressure points. The figure shows that less than 30 min is needed to reach equilibrium. Nevertheless, all samples were stored in a chamber for an hour before each change of pressure to insure equilibrium was reached. Furthermore, the decrease in the channel current with hydration indicates that the PEDOT:PSS is being hydrated, and incorporating passively diffusing protons from melanin into its matrix.

S4. References

SR1 D. A. Bernards, G. G. Malliaras, *Adv. Funct. Mater.*, 2007, **17**, 3538.

SR2 J. Rivnay, P. Leleux, M. Ferro, M. Sessolo, A. Williamson, D. A. Koutsouras, D. Khodagholy, M. Ramuz, X. Strakosas, R. M. Owens, C. Benar, J. M. Badier, C. Bernard, G. G. Malliaras, *Sci. Adv.*, 2015, **1**, e1400251.

SR3 A. B. Mostert, K. J. P. Davy, J. L. Ruggles, B. J. Powell, I. R. Gentle, P. Meredith, *Langmuir*, 2010, **26**, 412.

SR4 A. J. Clulow, A. B. Mostert, M. Sheliakina, A. Nelson, N. Booth, P. L. Burn, I. R. Gentle, P. Meredith, *Soft Matter*, 2017, **13**, 3954-3965.